ACS OMEGA

Article

Cite This: ACS Omega 2018, 3, 17439−17446

http://pubs.acs.org/journal/acsodf

Improving the Transport and Antifouling Properties of Poly(vinyl chloride) Hollow-Fiber Ultrafiltration Membranes by Incorporating Silica Nanoparticles

Sepehr Saberi,[†] Ahmad Arabi Shamsabadi,[‡] Mahdi Shahrooz,[†,§] Morteza Sadeghi,*[,§] and Masoud Soroush*[,‡]

[†]Tuka Parsian Pishro Co, Isfahan Science and Technology Town, Isfahan, Iran

[‡]Department of Chemical and Biological Engineering, Drexel University, Philadelphia, Pennsylvania 19104, United States

[§]Department of Chemical Engineering, Isfahan University of Technology, Isfahan 84156-83111, Iran

ABSTRACT: Poly(vinyl chloride) (PVC)/SiO_2 nanocomposite hollow-fiber membranes with different nano-SiO_2 particle loadings (0−5 wt %) were fabricated using the dry-jet wet-spinning technique. Effects of SiO_2 nanoparticles on the morphology of the prepared hollow-fiber membranes were investigated using scanning electron microscopy. Transport and antifouling properties of the fabricated membranes were evaluated by conducting pure-water permeation, solute rejection, and fouling resistance experiments. These studies indicated that incorporating silica nanoparticles into the PVC matrix during phase inversion lowers the hydraulic resistance through the membrane and narrows the selective membrane pores. Moreover, the nanocomposite membranes showed better antifouling properties compared to the pristine membrane during the ultrafiltration of a milk solution because of improved hydrophilicity and uniform dispersion of the nanoparticles. This work indicates that embedding silica nanoparticles into the PVC matrix is a promising method for producing cost-effective hollow-fiber ultrafiltration membranes with superior transport and antifouling properties.

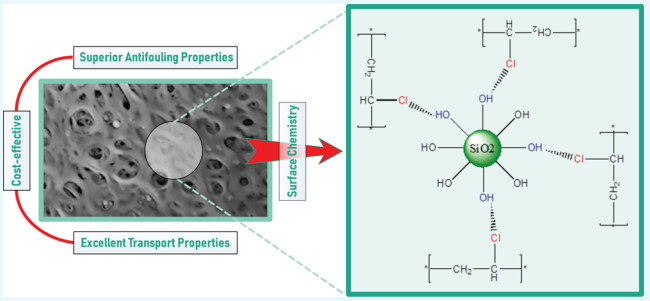

1. INTRODUCTION

Ultrafiltration is a low-pressure membrane process widely used for separation and purification of various compounds and streams in the food, pharmaceutical, biotechnology, and water-treatment industries.[1−5] Among polymers used in the fabrication of ultrafiltration membranes, poly(vinyl chloride) (PVC) is attractive for its favorable chemical resistance, mechanical properties, and lower price compared to polysulfone (PSF), polyethersulfone (PES), and polyvinylidine-flouride (PVDF).[6] These advantages have motivated studies on its application for polymer membrane fabrication.[7,8] However, its hydrophobicity promotes membrane fouling, restricting its application in water purification.[7,8] Membrane fouling lowers the flux and efficiency of membrane separation processes,[9−11] which have to be regained by chemical cleaning. However, chemical cleaning increases operating costs and lowers the membrane lifetime. As such, the fabrication of membranes with superior antifouling properties is of great importance.[12−14]

Physical blending,[15−18] chemical grafting,[19,20] and surface modification[21−23] are among the techniques utilized for improving membrane hydrophilicity, and thereby antifouling properties of ultrafiltration membranes. For instance, Panda and De[17] investigated how characteristics of the PSF ultrafiltration membranes are changed with adding polyethyleneglycol (PEG) to the dope solutions. They reported that an increase in the concentration and/or molecular weight of PEG promoted the hydrophilicity and consequently antifouling properties of the resulting hollow fibers. In another study, Zhao et al.[20] grafted *n*-isopropylacrylamide on the surface of PVDF membranes and created thermoresponsive membranes with improved hydrophilicity, fouling resistance, and pure water flux (PWF). Additionally, Abedi et al.[21,22] significantly improved the fouling resistance of polyacrilonitrile (PAN) membranes using chemical surface modification.

In recent years, the use of nanomaterials in the fabrication of polymer membranes has attracted a lot of interest because of improved performance of nanomaterial-based membranes.[24−27] Yang et al.[28] showed that the addition of 2 wt % TiO_2 to a PSF solution significantly enhances the PWF, hydrophilicity, mechanical strength, and fouling resistance, whereas solute rejection remained essentially unchanged. Yan et al.[29] employed PVDF/alumina ultrafiltration membranes for oil waste water treatment. The modified membranes exhibited improved fouling resistance, and in some cases, the flux recovery reached 100% after the chemical cleaning. SiO_2 nanoparticles have been used widely because of their low

Received: August 29, 2018
Accepted: October 24, 2018
Published: December 17, 2018

DOI: 10.1021/acsomega.8b02211
ACS Omega 2018, 3, 17439−17446

cost, ease of preparation, excellent stability, and hydrophilicity.[8,30,31] Shen et al.[31] studied PES/SiO_2 nanocomposite membranes for raw water pretreatment. Their results suggested that the morphology of the membranes was not affected significantly, whereas hydrophilicity and antifouling properties were improved.[31] Arthanareeswaran et al.[32] investigated the effect of silica on cellulose acetate (CA) membranes. The porosity and the mechanical strength of the CA membranes were found to improve with incorporating silica nanoparticles. Also, Jin et al.[33] found that silica nanoparticles enhanced thermal resistance, hydrophilicity, and flux of the ultrafiltration membranes. Harun et al.[34] investigated the effect of synthetic silica with different concentrations on the morphology and performance of PSF membranes. By embedding 2 wt % of silica a high PWF and a high solute rejection were achieved simultaneously. Yu et al.[35] reported that the membranes containing silica showed better performance in terms of permeability, fouling resistance, and solute separation.

Previous studies on the use of silica nanoparticles as fillers and pore-forming agents in PVC membranes have focused mostly on flat-sheet membranes.[8,36] As fabrication processes of flat-sheet and hollow-fiber membranes are governed by different nonsolvent-induced phase separation mechanisms, leading to the fabrication of membranes with different properties and structures.[37] Therefore, our understanding of flat-sheet membranes cannot be applied to hollow fibers, in general.[37]

This paper presents a study of the effects of silica nanoparticles on the morphology and performance of PVC hollow-fiber ultrafiltration membranes. Silica nanoparticles with various concentrations were incorporated into the PVC dope solutions. Subsequently, the solutions were spun into hollow fibers employing the dry-jet wet-spinning method. The resulting membranes were then characterized using thermal gravimetric analysis (TGA), scanning electron microscopy (SEM), and attenuated total reflectance Fourier transform infrared spectroscopy (ATR–FTIR), to observe the influence of silica nanoparticles on the morphology of the membranes. Furthermore, the separation performance of the ultrafiltration membranes was determined through measurement of PWF and solute rejection. Finally, fouling experiments were performed to evaluate the fouling resistance of the membranes against milk as a model foulant.

2. RESULTS AND DISCUSSION

2.1. ATR–FTIR and TGA. The silica nanoparticles may leave the membrane matrix during the spinning process. To confirm that this did not occur, ATR–FTIR analysis was performed. This analysis allows for qualitatively determining the percent of nanoparticles trapped in the membrane network (Figure 1), where the M-0.0, ..., M-5.0 are defined in Table 1. The strong absorption band at 1104 cm^{-1} corresponds to the asymmetric Si–O–Si stretching, corroborating the presence of the nanoparticles within the membrane matrix. Additionally, as the SiO_2 content increases from 0.5 to 5 wt %, the relative absorption intensity increases as well. This implies that the percent of SiO_2 nanoparticles trapped within the membrane structure enhances with its concentration in the initial dope solution.

To determine the percent of the nanoparticles trapped in the membrane network, TGA was carried out (Figure 2). Char yields of 13.84, 15.61, and 18.43% were observed for M-0.0, M-2.5, and M-5.0 up to 600 °C, respectively. Considering 4% loss of the silica weight loss up to this temperature,[38] silica concentrations of 1.84 and 4.78% were obtained for M-2.5 and M-5.0 samples, respectively.

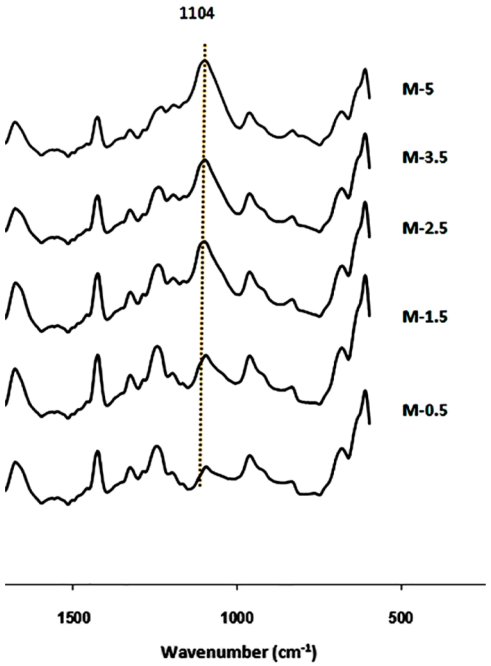

Figure 1. ATR–FTIR spectra of the modified PVC hollow-fiber membranes.

Table 1. Names Given to the Fabricated Membranes Based on Their Silica Concentration

sample	SiO_2 (%)
M-0.0	0.0
M-0.5	0.5
M-1.5	1.5
M-2.5	2.5
M-3.5	3.5
M-5.0	5.0

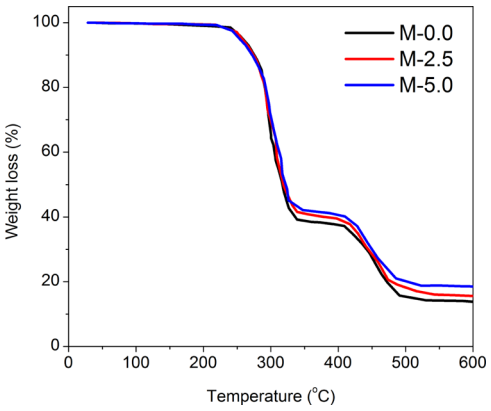

Figure 2. TGA thermographs of the fabricated membranes.

2.2. Effect of Silica Nanoparticles on Membrane Morphology. Cross-sectional images of the hollow-fiber membranes are presented in Figure 3. Three main regions including the lumen side surface, the middle region, and the outer surface were observed in the cross sections of the hollow fibers. The addition of silica nanoparticles to the PVC matrix led to an increase in porosity of the middle region.

DOI: 10.1021/acsomega.8b02211
ACS Omega 2018, 3, 17439–17446

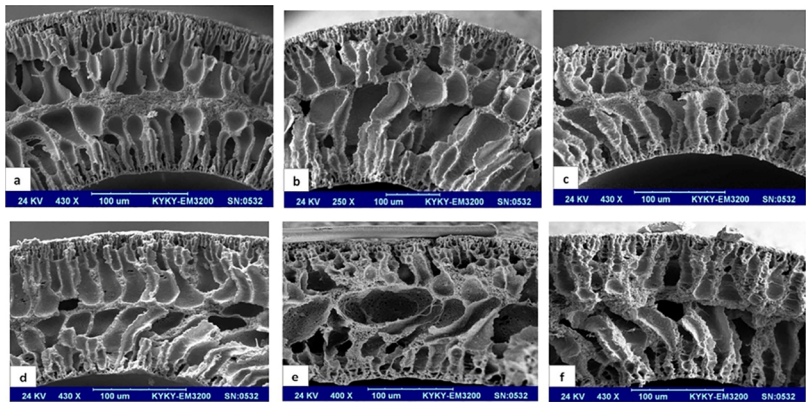

Figure 3. Cross-sectional images of the PVC/SiO_2 hollow-fiber membranes with (a) 0.0, (b) 0.5, (c) 1.5, (d) 2.5, (e) 3.5, and (f) 5.0 wt % SiO_2.

Additionally, the cross-section morphology appears to become coarser with increasing the percent of silica nanoparticles. As the polymer solution comes into contact with each of the internal (bore liquid) and external (coagulation bath) coagulation liquids, a high number of polymer-lean nuclei are formed in both the lumen side and the outer side of the hollow fiber, leading to the phase separation of the polymer solution. The initial nuclei grow until the gelation (or vitrification) point. Additionally, the rate of phase separation in these two surfaces, especially in the outer surface, is significantly higher than that in the bulk because of the presence of large amounts of nonsolvents close to both surfaces contacting the coagulation liquids. Therefore, due to the availability of less time for pore growth, the average size of the final pores on the surface, which are the result of nucleation and growth of the polymer-lean microdomains in the polymer-rich phase, is smaller than that of the bulk.

Because of the different compositions of the coagulation liquids in the lumen and outer sides, the porosity and the specification of the pores in these layers are different (Figure 4). Compared to the lumen side, a tighter and thicker layer was

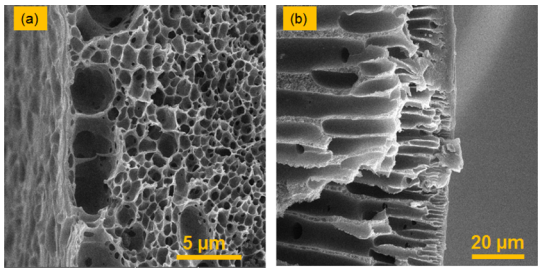

Figure 4. SEM images of the (a) lumen surface and (b) outer surface of the M-2.5 hollow-fiber membrane.

observed in the outer surface. A high amount of the solvent [dimethylformamide (DMF)] in the bore liquid led to a lower driving force for precipitation of the polymer in the lumen side, constructing a layer with more porosity and larger connected pores. Furthermore, the presence of DMF in the bore liquid slowed the phase inversion in the lumen side and allowed more nuclei growth. The transport of the nonsolvent molecules from the inner layer to the middle layer increased the porosity of the lumen layer.

As the phase separation advances toward the middle of the hollow-fiber bulk, the resistance in the outer and inner surfaces of the hollow fiber hinders the diffusion of the coagulant into the inner layers. Therefore, the rate of phase separation in this region is relatively low, and the polymer-lean nuclei formed in this region subsequently form large macrovoids.[8,35,39] The resistance of the outer and lumen side of the hollow fibers hinders diffusion of water into the middle layer. Therefore, in this layer, the nonsolvent concentration increases gradually, minimizing the rate of phase separation in the middle layer. The nuclei in this layer do not grow significantly because of the pressure exerted on this layer by the adjacent large finger-like nuclei. Therefore, a sponge-like morphology is observed in this layer.[8,40,41]

Silica nanoparticles act as nucleation sites because of their hydrophilic nature.[42] Therefore, by incorporation of these nanoparticles into the polymer solutions, the number of the nuclei and the rate of phase separation increase drastically, with ensuing smaller size of the final domains in both the lumen and outer surface of the hollow fibers. This phenomenon also takes place across the bulk of the hollow fibers; the presence of silica nanoparticles enhances the nucleation in the bulk of the dope solution. Therefore, the number of nuclei in the internal layers increases, resulting in smaller but interconnected macrovoids compared to the pure PVC hollow fiber. Additionally, because of the presence of the silica nanoparticles, the phase separation in the middle regions occurs more homogenously, engendering the suppression of the middle dense layer. As a result, the relatively dense middle layer, which exists in the pure PVC membranes, becomes looser.

Figure 5 presents the cross-section micrographs of the PVC/SiO_2 membranes at a higher magnification. It can be observed that the silica nanoparticles are distributed uniformly throughout the cross-section, verifying the compatibility of the PVC and SiO_2 nanoparticles. The hydroxyl groups on the surface of the nanoparticles and the Cl groups of the PVC chains can have polar interactions (Scheme 1).[43,44] These interfacial interactions improve the compatibility of the organic and inorganic phases.[45] However, with an increase in the concentration of the nanoparticles, the nanoparticles tend to agglomerate. The agglomerated silica nanoparticles were enclosed in the coarse pores on the cavity walls, blocking some of the pores almost completely (especially in M-5). This leads to a reduction in the connectivity between the macrovoids. The agglomeration of the silica nanoparticles is further amplified at higher nanoparticle concentrations by their hydrophilic nature and their tendency for phase separation from the polymer solution.

DOI: 10.1021/acsomega.8b02211
ACS Omega 2018, 3, 17439−17446

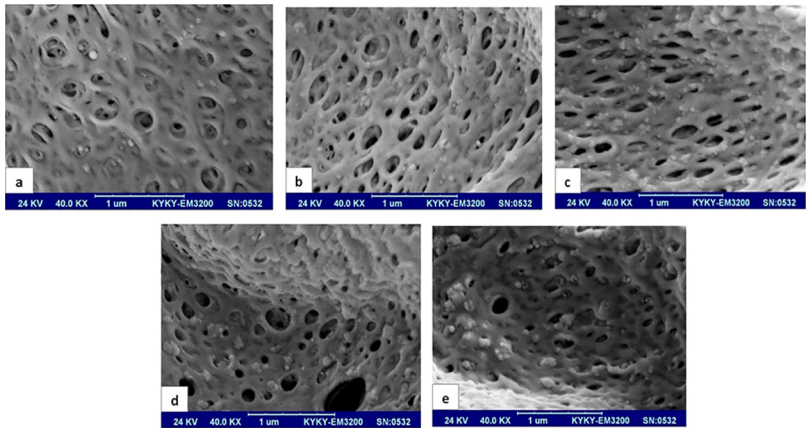

Figure 5. Cross-sectional SEM images of the PVC/SiO_2 membranes with (a) 0.5, (b) 1.5, (c) 2.5, (d) 3.5, and (e) 5.0 wt % SiO_2.

Scheme 1. Dispersion of SiO_2 Nanoparticles in PVC, and Possible Polar Interactions between the PVC Backbone and the Nanoparticles

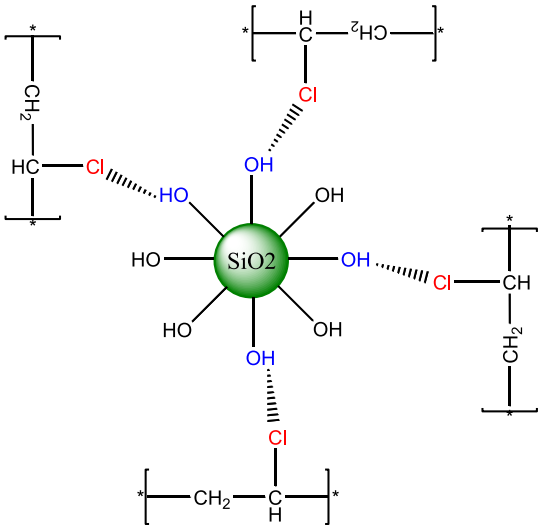

2.3. Effect of Silica Nanoparticles on the Performance of the Ultrafiltration Membranes. Solute rejection as well as PWF results are presented in Table 2. As the table shows, higher silica contents in the membranes provided higher solute rejections, indicating that the average size of the selective pores decreased. Increasing PWF seems counterintuitive at first sight, which can be attributed to the morphology of the membranes described before.

Table 2. PWF and Solute Rejection of the PVC/SiO_2 Membranes

		rejection (%)		
sample	PWF ($L \cdot m^{-2} \cdot h^{-1}$)	PVA (30 kDa)	PVA (60 kDa)	PVA (145 kDa)
M-0.0	99 ± 3	23	70	80
M-0.5	117 ± 4	23	77	100
M-1.5	126 ± 2	30	80	100
M-2.5	133 ± 2	36	85	100
M-3.5	137 ± 2	40	85	100
M-5.0	87 ± 1	40	83	100

The improved rejection of the tested solutes indicated a decrease in the average size of the selective pores. As described in the previous section, the presence of the silica nanoparticles in the polymer solution results in a higher number of nuclei in the phase separation process. This leads to a higher number of final pores with smaller size, which subsequently results in a higher rejection.[8] On the other hand, increasing the nanoparticle content creates a looser internal structure in the membranes, which consequently decreases the hydraulic resistance against the water transport through the membranes.[46] Therefore, the increase in PWF with nanoparticle content can be attributed to the decrease in the hydraulic resistance of the membrane bulk against water transport during the ultrafiltration process as a result of the formation of a higher number of interconnected pores. On the other side, improving solute rejection can be related to the decrease in pore size on the selective surface (in our case, the outer surface) of the membranes. It should also be noted that the decrease in the value of PWF from M-3.5 to M-5.0 can be ascribed to the increased hydraulic resistance against the water transport through the membranes as a result of the blockage of the coarse pores across the membrane bulk by the agglomerated nanoparticles.[46] In addition to the hydraulic resistance effect, the presence of OH groups on the surface of the silica nanoparticles improves the hydrophilicity of the membranes, leading to higher PWFs for the membranes that contain more nanoparticles (Figure 6), thereby facilitating the water transport through the pores. The M-3.5 membrane rejects poly(vinyl alcohol) (PVA) 30 kDa slightly more than

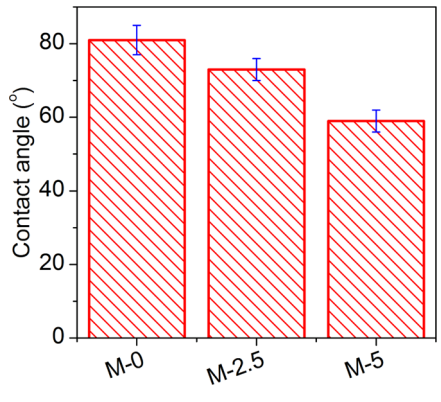

Figure 6. Water contact angles of the fabricated membranes.

DOI: 10.1021/acsomega.8b02211
ACS Omega 2018, 3, 17439−17446

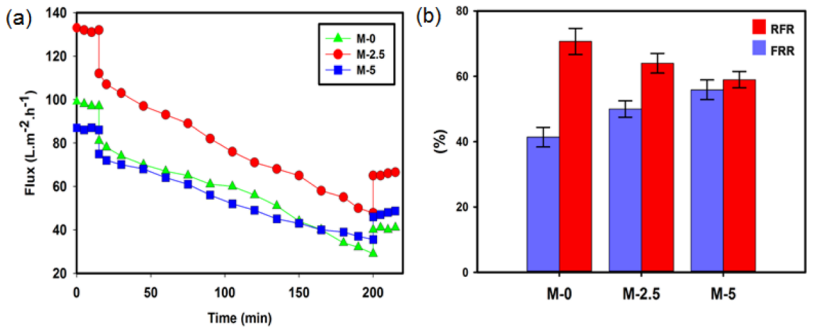

Figure 7. (a) Milk ultrafiltration flux vs time for the pristine and modified membranes and (b) changes of FRR and RFR for the pristine and modified membranes.

the M-2.5 membrane, whereas the two membranes reject PVA 60 kDa and PVA 145 kDa similarly. Also, M-3.5 showed a slightly higher PWF than M-2.5. Although the flux and rejection of M-3.5 is a slightly higher than those of the M-2.5, M-2.5 was selected as the best membrane to compare its antifouling properties with those of M-5.0 because of its easier fabrication process (easier mixing of the less nanoparticles in the polymer dope).

2.4. Effect of Nano-Silica on the Antifouling Performance of the Prepared Membranes. To evaluate the antifouling properties of the modified membranes, the prepared membranes containing 0.0, 2.5, and 5.0 wt % silica were examined in the milk ultrafiltration experiments. After 3 h of filtration of milk and cleaning of the tested membranes, the water flux of the cleaned membranes was measured. Figure 7 depicts the milk ultrafiltration flux as a function of time as well as the flux recovery ratio (FRR) and relative flux reduction (RFR) results.

As can be observed from Figure 7a,b, the value of RFR decreased with embedding silica nanoparticles, indicating the better resistance of the nanocomposite membranes against fouling in the presence of milk. This can be attributed to the presence of hydrophilic functional groups on the surface of the silica nanoparticles, which increases the hydrophilicity of the membranes (Figure 6), and consequently decreases the adhesion of the milk proteins to the membrane surface. Moreover, according to Figure 7b, FRR increases with the incorporation of silica nanoparticles, showing a decrease in irreversible fouling in the studied membranes. As described above, because of the reduced affinity between the membrane surface and the milk proteins, the adhered proteins were more easily removed from the membranes, decreasing the irreversible fouling. The improved antifouling properties can be attributed to the increase in connectivity of the macrovoids in the presence of the silica nanoparticles. The coarse structure facilitates the removal of foulant from the membrane bulk by enhancing the internal hydraulic flow across the membrane. Antifouling properties of the PVC/SiO_2 membranes are compared with other silica-based ultrafiltration membranes reported in the literature, in Table 3. Bovine serum albumin (BSA), PEG, and PVA solutions were used as foulant models. As can be seen in the table, PAN/SiO_2 and PVC/SiO_2 membranes rejected more than 80% of PEG 1000 and PVA 60 kDa, respectively. An almost complete rejection of higher-molecular-weight foulants was attained for these membranes. Furthermore, high BSA rejections of more than 92% were observed for the silica-based nanocomposite membranes.

Table 3. Antifouling Properties of the Silica-Based Membranes

membrane	filler content (wt %)	foulant type	rejection (%)	references
PES/SiO_2	2.0	BSA	96.1	40
PES/SiO_2/PVP	0.2	BSA	100	47
PES/SiO_2	1.5	BSA	92.6	48
PAN/SiO_2		PEG 1000	81.0	49
PAN/SiO_2		PEG 6000	99.0	49
PAN/SiO_2		BSA	100.0	49
PSF/SiO_2	1	BSA	95.0	50
PVC/SiO_2	2.5	PVA 60 kDa	85.0	this work
PVC/SiO_2	2.5	PVA 145 kDa	100.0	this work

3. CONCLUSIONS

Defect-free hollow-fiber ultrafiltration membranes were successfully fabricated by embedding silica nanoparticles into the PVC matrix using the dry-jet wet-spinning technique. Silica nanoparticles significantly affected the morphology as well as the transport and antifouling properties of the PVC membranes. The results suggest that the incorporation of silica nanoparticles increased the number of nuclei in the phase separation, leading to a decrease in the average size of the pores. As a result, a higher solute rejection was achieved thanks to the silica nanoparticles in the membrane network. Additionally, the modified membranes demonstrated higher PWFs compared to the pristine membrane because of their looser internal structures. However, increasing the nanoparticle content beyond a certain concentration (~3.5 wt %) decreased the PWF because of the agglomeration of the nanoparticles and pore blockage. Fouling experiments revealed that the positive effects of the nanoparticles on membrane hydrophilicity provided better antifouling properties for the nanocomposite membranes. This study points to the great potential of the silica nanoparticles to defy high fouling of the PVC ultrafiltration membranes as a major challenge of these membranes.

4. EXPERIMENTAL SECTION

4.1. Materials. PVC (grade: S-65) was supplied by Abadan Petrochemical Co., Abadan, Iran, and was dried at 70 °C for 30 min before use. DMF was purchased from Aldrich and was used as the solvent for preparation of the polymer dopes. SiO_2 nanoparticles with a mean particle size of 15 nm were purchased from TECNAM, Italy. Poly(vinyl pyrrolidone) (PVP-K90) was purchased from Rahavard Tamin Co., Tehran, Iran, and was utilized as an additive in preparing the dope

DOI: 10.1021/acsomega.8b02211
ACS Omega 2018, 3, 17439−17446

solutions. PVA with molecular weights of 30, 60, and 145 kDa was obtained from Merck, Germany, to evaluate the solute rejection of the membranes.

4.2. Membrane Preparation. For preparation of the dope solutions, silica nanoparticles with various concentrations were dispersed in the solvent (DMF) via bath-ultrasonicating for 2 h at room temperature. PVC and PVP were then gradually added to the suspension followed by 24 h rigorous stirring and ultrasonicating to obtain a homogeneous dope solution. The compositions of the dope solutions and names of the corresponding fabricated membranes are listed in Table 4.

Table 4. Compositions of the Dope Solutions and Names of the Corresponding Membranes

sample	PVC (%)	PVP (%)	DMF (%)	SiO_2 (%)
M-0.0	20	3	77.0	0.0
M-0.5	20	3	76.5	0.5
M-1.5	20	3	75.5	1.5
M-2.5	20	3	74.5	2.5
M-3.5	20	3	73.5	3.5
M-5.0	20	3	72.0	5.0

For the preparation of the PVC/SiO_2 nanocomposite hollow-fiber membranes, the dope solutions were spun by the dry-jet wet-spinning method at 25 °C. The bore liquid was a 15 wt % DMF aqueous solution. After leaving the spinneret and traveling a 25 cm air gap, the solution entered a coagulation bath containing pure water. Subsequently, the membranes were collected in a washing bath containing pure water. The fabricated hollow-fiber membranes were kept in a water bath for 24 h to remove the residual solvent, and subsequently were immersed into a tank containing a 20 wt % glycerol aqueous solution for 24 h to prevent the porous structure from collapsing. Finally, the membranes were dried at ambient air before conducting characterization and performance experiments. The spinning conditions are summarized in Table 5.

Table 5. Spinning Conditions for the Fabrication of the PVC/SiO_2 Hollow-Fiber Membranes

parameter	value
bore fluid (water/DMF) composition (wt/wt)	15/85
external coagulant	water
air−gap distance (cm)	25
dope flow rate (mL/min)	7
bore fluid flow rate (mL/min)	5
take-up speed (m/min)	9
coagulation bath temperature (°C)	40
spinneret dimensions (OD/ID) (mm/mm)	1.3/0.64

4.3. Membrane Characterization. *4.3.1. SEM, ATR−FTIR, TGA, and Contact Angle Analyses.* The morphologies of the prepared membranes were examined using a SEM (KYKY, model: EM3200, China). The membrane samples were fractured in liquid nitrogen and were gold-coated before visualization. ATR−FTIR analysis of the samples was performed using a Bruker TENSOR 27, IR spectrometer in the wavenumber range of 4000−600 cm^{-1}. Prior to the experiments, the samples were placed in a vacuum oven to remove the residual moisture. To quantify the silica content of the membranes, TGA was performed with a thermogravimetric analyzer (model TA Instruments TGA Q50) under ultrahigh pure nitrogen and a heating rate of 10 °C/min. A ramé-hat automated goniometer (model 290-U1) was employed to measure contact angles of the membranes. Deionized water (3 μL) was dropped on the membranes by a microsyringe at 25 °C. Five independent measurements were made for each case; the average of the five measurements is reported for each case in this paper.

4.3.2. Membrane Performance Test. Flux and fouling experiments were carried out using the setup shown in Scheme 2. For all performance experiments, the membranes of each group were placed in a module using epoxy resin. Each module contained eight hollow-fiber filaments. The effective length of the filaments in each module was 20 cm, providing an active membrane surface area of about 65 cm^2. In all of the tests, the flow configuration of the feed solution was set in "out-to-in" mode, that is, the outer surface of the membranes was exposed to the feed solution, and permeate was collected from the lumen side. All of the performance experiments were carried out at ambient temperature (25 ± 1 °C).

4.3.2.1. Pure-Water Flux. Before the PWF experiments, each module was pressurized with pure water at 3 bar for 30 min. After that, the upstream pressure was reduced and the experiments were performed at 2 bar. The permeate volume obtained in each experiment, V (L), was used for calculating the permeate flux, J ($L{\cdot}m^2{\cdot}h^{-1}$), using

$$J = \frac{V}{At} \tag{1}$$

where A (m^2) is the active surface area of the hollow fibers in the module and t (h) is the test time.

4.3.2.2. Fouling Experiment. Fouling experiments were performed to determine the impact of silica nanoparticles on the fouling resistance of the prepared membranes as well as their flux-recovery characteristics. Details of the utilized experimental procedure can be found in ref 22. In these experiments, permeation fluxes of a pure water and a milk solution (approximately 90.1 wt % water, 1.5 wt % fat, and 8.4 wt % nonfat solid) streams were measured. First, the PWF of the neat membranes was measured, followed by the measurement of the milk solution flux (which was used to create fouling in the samples). The PWF was measured again after backwashing the modules to remove the reversible fouling. The measured fluxes of the pure water before (J_w) and after (J_{wuf}) the milk filtration were subsequently used to determine the FRR using

$$\text{FRR}\ (\%) = 100\left(\frac{J_{wuf}}{J_w}\right) \tag{2}$$

Additionally, the permeation flux of the milk solution (J_p) was used to determine the RFR using

$$\text{RFR}\ (\%) = \left(1 - \frac{J_p}{J_w}\right)100 \tag{3}$$

The characteristics of the milk solution used for this study are identical to those reported in ref 22.

4.3.2.3. Solute Rejection Experiment. Solute rejection tests were performed using aqueous solutions of PVA with three different molecular weights of 30, 60, and 145 kDa at a concentration (C_f) of 0.4 wt % (4000 ppm), a pressure of 2 bar, and a temperature of 25 ± 1 °C. Details of the employed

DOI: 10.1021/acsomega.8b02211
ACS Omega 2018, 3, 17439−17446

Scheme 2. Schematic Representation of the Setup Used for Performing the Flux and Fouling Experiments

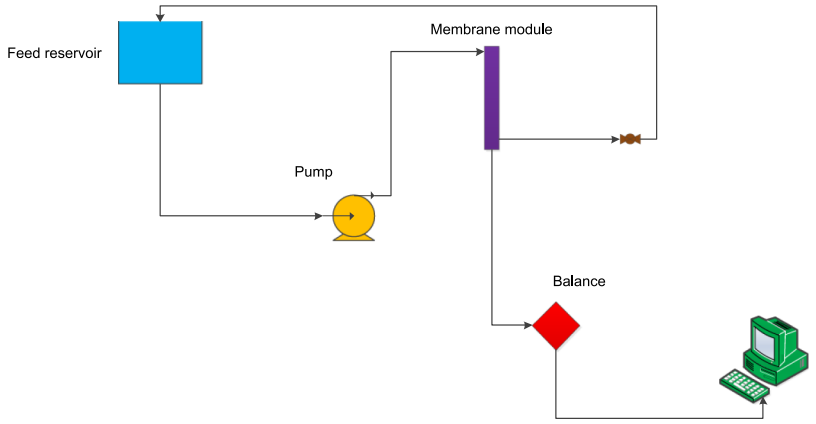

experimental procedure can be found in ref 22. The solute rejection, R (%), was calculated using[22]

$$R = \left(1 - \frac{C_p}{C_f}\right)100 \quad (4)$$

where C_p denotes the concentration of PVA in the permeate solution.

AUTHOR INFORMATION

Corresponding Authors

*E-mail: m-sadeghi@cc.iut.ac.ir (Morteza Sadeghi).
*E-mail: soroushm@drexel.edu (Masoud Soroush).

ORCID

Ahmad Arabi Shamsabadi: 0000-0002-9726-2466
Morteza Sadeghi: 0000-0002-0075-1520

Notes

The authors declare no competing financial interest.

ACKNOWLEDGMENTS

Ahmad A. Shamsabadi was partially supported by the U.S. National Science Foundation under Grant No. CBET−1804285.

REFERENCES

(1) Bao, W.; Xu, Z.; Yang, H. Electrokinetic and permeation characterization of hydrolyzed polyacrylonitrile (PAN) hollow fiber ultrafiltration membrane. *Sci. China, Ser. B: Chem.* **2009**, *52*, 683−689.

(2) Sadeghian, M.; Sadeghi, M.; Hesampour, M.; Moheb, A. Application of response surface methodology (RSM) to optimize operating conditions during ultrafiltration of oil-in-water emulsion. *Desalin. Water Treat.* **2015**, *55*, 615−623.

(3) Zhang, G.; Song, X.; Li, J.; Ji, S.; Liu, Z. Single-side hydrolysis of hollow fiber polyacrylonitrile membrane by an interfacial hydrolysis of a solvent-impregnated membrane. *J. Membr. Sci.* **2010**, *350*, 211−216.

(4) Mokhtari, S.; Rahimpour, A.; Shamsabadi, A. A.; Habibzadeh, S.; Soroush, M. Enhancing performance and surface antifouling properties of polysulfone ultrafiltration membranes with salicylate-alumoxane nanoparticles. *Appl. Surf. Sci.* **2017**, *393*, 93−102.

(5) Qin, Y.; Yang, H.; Xu, Z.; Li, F. Surface Modification of Polyacrylonitrile Membrane by Chemical Reaction and Physical Coating: Comparison between Static and Pore-Flowing Procedures. *ACS Omega* **2018**, *3*, 4231−4241.

(6) Ahmadpour, E.; Sarfaraz, M. V.; Behbahani, R. M.; Shamsabadi, A. A.; Aghajani, M. Fabrication of mixed matrix membranes containing TiO_2 nanoparticles in Pebax 1657 as a copolymer on an ultra-porous PVC support. *J. Nat. Gas Sci. Eng.* **2016**, *35*, 33−41.

(7) Xu, J.; Xu, Z.-L. Poly (vinyl chloride)(PVC) hollow fiber ultrafiltration membranes prepared from PVC/additives/solvent. *J. Membr. Sci.* **2002**, *208*, 203−212.

(8) Yu, Z.; Liu, X.; Zhao, F.; Liang, X.; Tian, Y. Fabrication of a low-cost nano-SiO_2/PVC composite ultrafiltration membrane and its antifouling performance. *J. Appl. Polym. Sci.* **2015**, *132*, 41267.

(9) Rahimpour, A.; Seyedpour, S. F.; Aktij, S. A.; Firouzjaei, M. D.; Zirehpour, A.; Shamsabadi, A. A.; Salestan, S. K.; Jabbari, M.; Soroush, M. Simultaneous Improvement of Antimicrobial, Antifouling, and Transport Properties of Forward Osmosis Membranes with Immobilized Highly-Compatible Polyrhodanine Nanoparticles. *Environ. Sci. Technol.* **2018**, *52*, 5246−5258.

(10) Zirehpour, A.; Rahimpour, A.; Shamsabadi, A. A.; Sharifian Gh, M.; Soroush, M. Mitigation of thin-film composite membrane biofouling via immobilizing nano-sized biocidal reservoirs in the membrane active layer. *Environ. Sci. Technol.* **2017**, *51*, 5511−5522.

(11) Mohanraj, G.; Mao, C.; Armine, A.; Kasher, R.; Arnusch, C. J. Ink-Jet Printing-Assisted Modification on Polyethersulfone Membranes Using a UV-Reactive Antimicrobial Peptide for Fouling-Resistant Surfaces. *ACS Omega* **2018**, *3*, 8752−8759.

(12) Qiao, X.; Zhang, Z.; Ping, Z. Hydrophilic modification of ultrafiltration membranes and their application in Salvia Miltiorrhiza decoction. *Separ. Purif. Technol.* **2007**, *56*, 265−269.

(13) Zhao, X.; Su, Y.; Chen, W.; Peng, J.; Jiang, Z. Grafting perfluoroalkyl groups onto polyacrylonitrile membrane surface for improved fouling release property. *J. Membr. Sci.* **2012**, *415−416*, 824−834.

(14) Madaeni, S. S.; Vatanpour, V.; Monfared, H. A.; Shamsabadi, A. A.; Majdian, K.; Laki, S. Removal of coke particles from oil contaminated marun petrochemical wastewater using PVDF microfiltration membrane. *Ind. Eng. Chem. Res.* **2011**, *50*, 11712−11719.

(15) Maheswari, P.; Barghava, P.; Mohan, D. Preparation, morphology, hydrophilicity and performance of poly (ether-ether-sulfone) incorporated cellulose acetate ultrafiltration membranes. *J. Polym. Res.* **2013**, *20*, 74.

(16) Mansourizadeh, A.; Azad, A. J. Preparation of blend polyethersulfone/cellulose acetate/polyethylene glycol asymmetric membranes for oil−water separation. *J. Polym. Res.* **2014**, *21*, 375.

(17) Panda, S. R.; De, S. Role of polyethylene glycol with different solvents for tailor-made polysulfone membranes. *J. Polym. Res.* **2013**, *20*, 179.

(18) Shekarian, E.; Saljoughi, E.; Naderi, A. Polyacrylonitrile (PAN)/IGEPAL blend asymmetric membranes: preparation, morphology, and performance. *J. Polym. Res.* **2013**, *20*, 162.

(19) Nazri, N. A. M.; Lau, W. J.; Padaki, M.; Ismail, A. F. A facile modification approach for polyacrylonitrile-based UF hollow fiber membrane utilizing polyacrylonitrile-g-poly (vinyl alcohol) graft copolymer. *J. Polym. Res.* **2014**, *21*, 594.

DOI: 10.1021/acsomega.8b02211
ACS Omega 2018, 3, 17439−17446

(20) Zhao, Y.; Zhao, H.; Chen, L.; Feng, X.; Zhang, Q.; Wang, J.; Zhang, R. Thermo-responsive modification and properties study of PVDF flat membrane. *J. Polym. Res.* **2013**, *20*, 58.
(21) Abedi, M.; Chenar, M. P.; Sadeghi, M. Surface modification of PAN hollow fiber membrane by chemical reaction. *Fibers Polym.* **2015**, *16*, 788−793.
(22) Abedi, M.; Sadeghi, M.; Chenar, M. P. Improving antifouling performance of PAN hollow fiber membrane using surface modification method. *J. Taiwan Inst. Chem. Eng.* **2015**, *55*, 42−48.
(23) Yang, M.-C.; Lin, W.-C. Ultrafiltration of myoglobin using surface-sulfonated polysulfone hollow fiber. *J. Polym. Res.* **2002**, *9*, 61−67.
(24) Goh, P. S.; Ng, B. C.; Lau, W. J.; Ismail, A. F. Inorganic nanomaterials in polymeric ultrafiltration membranes for water treatment. *Separ. Purif. Rev.* **2015**, *44*, 216−249.
(25) Kim, J.; Van der Bruggen, B. The use of nanoparticles in polymeric and ceramic membrane structures: review of manufacturing procedures and performance improvement for water treatment. *Environ. Pollut.* **2010**, *158*, 2335−2349.
(26) Ng, L. Y.; Mohammad, A. W.; Leo, C. P.; Hilal, N. Polymeric membranes incorporated with metal/metal oxide nanoparticles: a comprehensive review. *Desalination* **2013**, *308*, 15−33.
(27) Zhao, X.; Zhang, W.; Chen, S.; Zhang, J.; Wang, X. Hydrophilicity and crystallization behavior of PVDF/PMMA/TiO_2 (SiO_2) composites prepared by in situ polymerization. *J. Polym. Res.* **2012**, *19*, 9862.
(28) Yang, Y.; Zhang, H.; Wang, P.; Zheng, Q.; Li, J. The influence of nano-sized TiO_2 fillers on the morphologies and properties of PSF UF membrane. *J. Membr. Sci.* **2007**, *288*, 231−238.
(29) Yan, L.; Li, Y. S.; Xiang, C. B. Preparation of poly (vinylidene fluoride)(pvdf) ultrafiltration membrane modified by nano-sized alumina (Al_2O_3) and its antifouling research. *Polymer* **2005**, *46*, 7701−7706.
(30) Mohagheghian, M.; Sadeghi, M.; Chenar, M. P.; Naghsh, M. Gas separation properties of polyvinylchloride (PVC)-silica nano-composite membrane. *Korean J. Chem. Eng.* **2014**, *31*, 2041−2050.
(31) Shen, J.-n.; Ruan, H.-m.; Wu, L.-g.; Gao, C.-j. Preparation and characterization of PES−SiO_2 organic−inorganic composite ultra-filtration membrane for raw water pretreatment. *Chem. Eng. J.* **2011**, *168*, 1272−1278.
(32) Arthanareeswaran, G.; Sriyamunadevi, T.; Raajenthiren, M. Effect of silica particles on cellulose acetate blend ultrafiltration membranes: Part I. *Sep. Purif. Technol.* **2008**, *64*, 38−47.
(33) Jin, L.; Shi, W.; Yu, S.; Yi, X.; Sun, N.; Ma, C.; Liu, Y. Preparation and characterization of a novel PA-SiO_2 nanofiltration membrane for raw water treatment. *Desalination* **2012**, *298*, 34−41.
(34) Harun, Z.; Jamalludin, M. R.; Basri, H.; Shohur, M. F.; Rosman, N.; Yunos, M. Z. The effect of synthetic silica on ultrafiltration PSf membrane. *J. Teknol.* **2013**, *65*, 121.
(35) Yu, L.-Y.; Xu, Z.-L.; Shen, H.-M.; Yang, H. Preparation and characterization of PVDF−SiO_2 composite hollow fiber UF membrane by sol−gel method. *J. Membr. Sci.* **2009**, *337*, 257−265.
(36) Zhao, F.-B.; Yu, Z.-J.; Park, H.-D.; Liu, X.-Y.; Song, X.-R.; Li, Z.-S. Polyvinylchloride Ultrafiltration Membranes Modified with Different SiO_2 Particles and Their Antifouling Mechanism for Oil Extraction Wastewater. *J. Environ. Eng.* **2015**, *141*, 04015009.
(37) Peng, N.; Widjojo, N.; Sukitpaneenit, P.; Teoh, M. M.; Lipscomb, G. G.; Chung, T.-S.; Lai, J.-Y. Evolution of polymeric hollow fibers as sustainable technologies: past, present, and future. *Prog. Polym. Sci.* **2012**, *37*, 1401−1424.
(38) Lin, B.; Zhou, S. Poly (ethylene glycol)-grafted silica nanoparticles for highly hydrophilic acrylic-based polyurethane coatings. *Prog. Org. Coat.* **2017**, *106*, 145−154.
(39) Saedi, S.; Madaeni, S. S.; Shamsabadi, A. A. Fabrication of asymmetric polyethersulfone membranes for separation of carbon dioxide from methane using polyetherimide as polymeric additive. *Chem. Eng. Res. Des.* **2014**, *92*, 2431−2438.
(40) Huang, J.; Zhang, K.; Wang, K.; Xie, Z.; Ladewig, B.; Wang, H. Fabrication of polyethersulfone-mesoporous silica nanocomposite ultrafiltration membranes with antifouling properties. *J. Membr. Sci.* **2012**, *423−424*, 362−370.
(41) Saedi, S.; Nikravesh, B.; Seidi, F.; Moradi, L.; Shamsabadi, A. A.; Salarabadi, M. B.; Salimi, H. Facilitated transport of CO_2 through novel imidazole-containing chitosan derivative/PES membranes. *RSC Adv.* **2015**, *5*, 67299−67307.
(42) Xiu, H.; Huang, C.; Bai, H.; Jiang, J.; Chen, F.; Deng, H.; Wang, K.; Zhang, Q.; Fu, Q. Improving impact toughness of polylactide/poly (ether) urethane blends via designing the phase morphology assisted by hydrophilic silica nanoparticles. *Polymer* **2014**, *55*, 1593−1600.
(43) Sadeghi, M.; Shamsabadi, A. A.; Ronasi, A.; Isfahani, A. P.; Dinari, M.; Soroush, M. Engineering the Dispersion of Nanoparticles in Polyurethane Membranes to Control Membrane Physical and Transport Properties. *Chem. Eng. Sci.* **2018**, *192*, 688.
(44) Laki, S.; Shamsabadi, A. A.; Seidi, F.; Soroush, M. Sustainable Recovery of Silver from Deactivated Catalysts Using a Novel Process Combining Leaching and Emulsion Liquid Membrane Techniques. *Ind. Eng. Chem. Res.* **2018**, *57*, 13821.
(45) Shamsabadi, A. A.; Seidi, F.; Salehi, E.; Nozari, M.; Rahimpour, A.; Soroush, M. Efficient CO_2 removal using novel mixed-matrix membranes with modified TiO_2 nanoparticles. *J. Mater. Chem. A* **2017**, *5*, 4011−4025.
(46) Cui, A.; Liu, Z.; Xiao, C.; Zhang, Y. Effect of micro-sized SiO_2 particle on the performance of PVDF blend membranes via TIPS. *J. Membr. Sci.* **2010**, *360*, 259−264.
(47) Sun, M.; Su, Y.; Mu, C.; Jiang, Z. Improved antifouling property of PES ultrafiltration membranes using additive of silica− PVP nanocomposite. *Ind. Eng. Chem. Res.* **2010**, *49*, 790−796.
(48) Li, Q.; Pan, S.; Li, X.; Liu, C.; Li, J.; Sun, X.; Shen, J.; Han, W.; Wang, L. Hollow mesoporous silica spheres/polyethersulfone composite ultrafiltration membrane with enhanced antifouling property. *Colloids Surf., A* **2015**, *487*, 180−189.
(49) Hu, Y.; Lü, Z.; Wei, C.; Yu, S.; Liu, M.; Gao, C. Separation and antifouling properties of hydrolyzed PAN hybrid membranes prepared via in-situ sol-gel SiO_2 nanoparticles growth. *J. Membr. Sci.* **2018**, *545*, 250−258.
(50) Habibi, S.; Nematollahzadeh, A., Enhanced water flux through ultrafiltration polysulfone membrane via addition-removal of silica nano-particles: Synthesis and characterization. *J. Appl. Polym. Sci.* **2016**, *133* (). DOI: 10.1002/app.43556

DOI: 10.1021/acsomega.8b02211
ACS Omega 2018, 3, 17439−17446